

---

---

ELECTROMAGNETIC METHODS

---

---

## Monitoring Stressed State of Pipelines by Magnetic Parameters of Metal

V. V. Filinov<sup>a, \*</sup>, A. N. Kuznetsov<sup>a, \*</sup>, and P. G. Arakelov<sup>b, \*\*</sup>

<sup>a</sup>Moscow Technological University (MIREA), Moscow, 119454 Russia

<sup>b</sup>Gazprom Gaznadzor, Moscow, 117418 Russia

\*e-mail: mgupir-4@mail.ru

\*\*e-mail: wargod\_venom@mail.ru

Received November 29, 2015; in final form, June 28, 2016

**Abstract**—A method is described for assessing the residual life of pipelines and articles made of structural steels. Dependences between applied stresses and parameters of registered magnetic noises are shown. Criteria are suggested for assessing the in-service destruction of pipeline metal by its magnetic parameters.

*Keywords:* magnetic noises, hysteresis loop parameters, estimating operating resource of pipelines

**DOI:** 10.1134/S1061830917010065

An in-service pipeline is subjected to a number of impacts that lead to the destruction of its metal. Due to the nonuniformity of these impacts over the pipeline length, the degree of metal destruction may reach critical values in certain zones, thus leading to pipeline destruction in these zones, with the rest of the pipeline staying in a perfectly operable condition. Increased dislocation density (reduction of metal plastic properties), formation of pores and microcracks (destruction elements), and metal corrosion can be called starting points for the emergence of destruction elements in pipeline metal.

With allowance for the weight of different factors that lead to the accelerated destruction of metal in local areas, it should be noted that the predominant role is played in this process by mechanical stresses that act in these areas of pipeline metal. Affected by the stresses, metal in these areas is subjected to ageing that leads to the accumulation of precipitate particles on the grain boundaries and to the processes of creep due to dislocation climb [1]. On the macroscopic level, this significantly reduces steel plasticity and, as a consequence, leads to the emergence of destruction and an increase in the likelihood of the pipeline brittle failure.

Experience has shown that, apart from metal plasticity reduction, pipeline failures are always accompanied by an increased level of local mechanical stresses acting inside metal. For example, analysis of data on failures in linear parts of long-distance pipelines in Western Siberia [3] shows that 27% of the failures were related to the action of longitudinal stresses and 13% to the action of circumferential (hoop) stresses.

These local stresses emerge in certain zones of pipelines for a number of reasons that are related to operating conditions (mechanical deformation of pipe walls, changes in the state of soil, temperature, etc.); the thinning of the walls, for example, due to metal corrosion; and others.

Search for the methods of nondestructive testing of pipelines and determining informative indicators for assessing their condition with the aim to allow as fully as possible for the effect of various factors on the in-service destruction of steel constructions and to create a methodology for evaluating the resource of the constructions never cease [5–7, 9, 10, 15, 16].

This article is concerned with the possibility for using parameters of magnetic nondestructive testing to reveal zones of metal destruction on in-service pipelines that operate under the action of applied stresses. The following goal was set when conducting the research: to choose parameters that, on the one hand, allow estimation of changes in the magnetic state of steel and, on the other hand, are related to the crystalline structure of steel and to changes it undergoes when loaded.

To this end, we applied a theory that is based on the notions about areas of spontaneous magnetization in ferromagnets (or domains [2, 4]). This theory provides the basis for such nondestructive testing methods as measurements of magnetic noises [4, 5, 7, 20] and coercimetry [2, 5, 11, 12, 14].

Changes in the structural properties of steels are closely related to changes in the magnetic texture. The method of magnetic noises (MN), which is based on measuring magnetization jumps (Barkhausen jumps, BJ) [4, 5], is the most promising technique for magnetic-texture estimation.

The power spectrum density that characterizes MN energy properties is known to be proportional to the product of the number of magnetization jumps per unit time and the square of the magnetic moment of a typical jump [4, 5]. The magnetic moment of a jump is determined by the energy of interaction between a domain wall and a crystal flaw and the distance that the wall covers in the jump, that is, by the density of flaws in the crystal. The number of magnetization jumps characterizes emission properties of MN and is determined by the number of acts of interaction between domain walls and structural flaws. The MN-induced emf obtained with PION and MSh devices is used in practice to estimate the level of magnetic noises [5, 8, 19, 20].

In [5], the shape of the envelope of magnetic noises (MNE) is analyzed versus the level of micro- and macroscopic stresses within the frame of the model of distribution of the critical BJ initiation fields  $H_0$  along the hysteresis curve  $B(H)$  in a quasistatic linear mode of magnetization reversal in a polycrystalline ferromagnet.

In this case, the equation of motion of an interdomain wall is of a stochastic nature, while the critical BJ start fields  $H_0$  are determined by a random function of the distribution of internal stresses  $\sigma$  in a polycrystalline ferromagnet. According to the Kersten–Kondorsky theory, the value of the critical field  $H_0$  is determined [2] as

$$H_0 \geq \frac{1}{2I_s} \sqrt{\frac{A}{K + \lambda_{100}\sigma_0}} \lambda \frac{d\sigma}{dx}, \quad (1)$$

where  $I_s$  is the saturation magnetization;  $A$  is the exchange energy constant;  $\lambda_{100}$  is the magnetostriction constant;  $K$  is the crystallographic anisotropy constant; and  $\sigma$  are mechanical stresses. Allowing for the type of the random function  $\sigma$  for high-strength steels, one can conclude that the quantity  $\sigma_0$  in the above expression is the mathematical expectation of this function and characterizes the level of macroscopic stresses, whereas the parameter  $d\sigma/dx \sim \sigma_x$  is its root-mean-square deviation that reflects the level of microscopic stresses.

Based on the theory of equilibrium statistical distributions [2, 5] and allowing for the canonical distribution and the above expression in Eq. (1), an expression was obtained for the function of distribution of critical fields in a three-dimensional “space of quantities”  $H_i$  for an anisotropic medium when the direction of action of macroscopic stresses coincides with the magnetization-reversal direction.

Analysis of the expression that determines the MNE shape and of its graphical interpretation demonstrated the expedience of using the informative parameters of the amplitude  $E_M$  and the field  $H_M$  of the MNE maximum,

$$H_M = \frac{2\alpha\lambda_{100}\sigma_x}{\sqrt{K_{\text{eff}}}}; \quad E_M = 0.34 \frac{\sqrt{K_{\text{eff}}} \exp\sqrt{K_{\text{eff}}/b}}{\lambda_{100}\sigma_x}, \quad (2)$$

when developing algorithms and techniques of testing, where  $K_{\text{eff}} = K + \lambda_{100}\sigma_0$  and  $C_0$ ,  $b$ , and  $a$  are dimension factors.

Figures 1 and 2 show experimental dependences of MNE on the level of tensile stresses  $\sigma_0$  and microstresses  $\sigma_x$  obtained by the method [5] that confirm the suggested MNE model. Analysis of the expression in Eq. (2) and the experimental dependences showed the following: tensile stresses lead to increase of  $E_M$  and decrease of  $H_M$  while compression stresses have an opposite effect; increasing the level of microstresses  $\sigma_x$  decreases the value of  $E_M$  and increases  $H_M$ .

The results obtained extend to include all structural steels such as carbon steels (20, 35, 50, 60), carbon alloyed steels (35X3HM, 30XГCH2A, 45X1, 45XH2MΦA), and high-alloy maraging steels (03H17K10B10MT, ЧC-98) [5].

The type of the dependence  $E = f(\sigma)$  of the half-period average value of MN emf on the value of the stresses  $\sigma$  is the same for different steel grades. By way of example, Fig. 3 shows calibrated graphs of the scale of the PION device [5] obtained when evaluating technological stresses in articles made of 03H17K10B10MT steel.

The graphs demonstrate a close-to-linear dependence between the values of mechanical stresses  $\sigma$  and the signal  $E$ , which is especially pronounced for tensile stresses. For small compression stresses (on the order of 100–200 MPa), a break of the graph is observed with a changeover to another linear dependence.

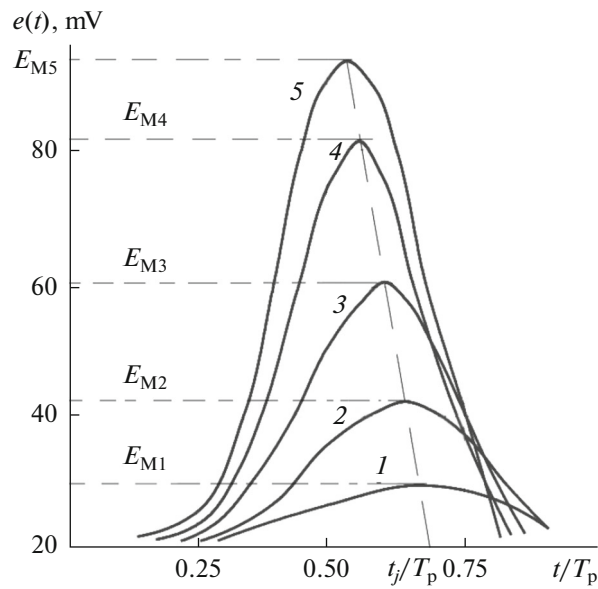


**Fig. 1.** Envelopes of MN ( $t_j/T$  is the ratio of the current time  $t$  to the magnetization-reversal signal period  $T_p$ ) for 30XГCH2A steel for different values of applied stresses,  $\sigma_0$ : (1) -200; (2) 0; (3) 200; (4) 400; (5) 600 MPa.

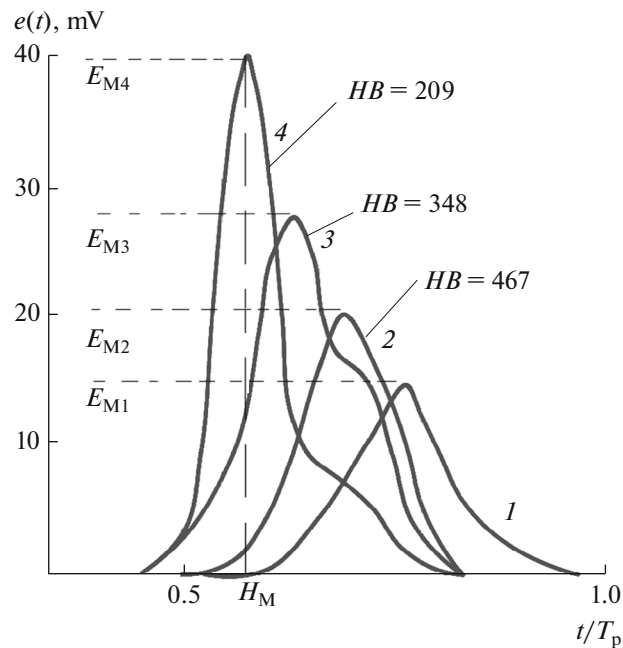


**Fig. 2.** Variation of MNE  $e(t)$  for 30XГCH2A steel after quenching at 900°C (1) and after quenching and tempering at 180 (2), 360 (3), and 540°C (4). HB is the Brinell hardness.

The sensitivity  $K$  toward stress change is  $K = \frac{\Delta E}{\Delta \sigma} \approx (4-5) \text{ mV/MPa}$  under tensile stresses and  $K = \frac{\Delta E}{\Delta \sigma} \approx (1.2-1.8) \text{ mV/MPa}$  under compression stresses (in what follows, we will define  $E$  in arbitrary units (a.u.) since the characteristics of measurement channels in different magnetic-noise devices are incompatible).

Experiments with different steels showed that the MN emf amplitude in the direction of applied load (along the magnetization axis) increases as this load grows while decreasing in the direction perpendicular to the direction of the load action. The relative change of the MN emf when detected in a sample across its loading axis comprises, on the average, a value of approximately 0.3 of the same change when detected along the loading axis for different steel grades.

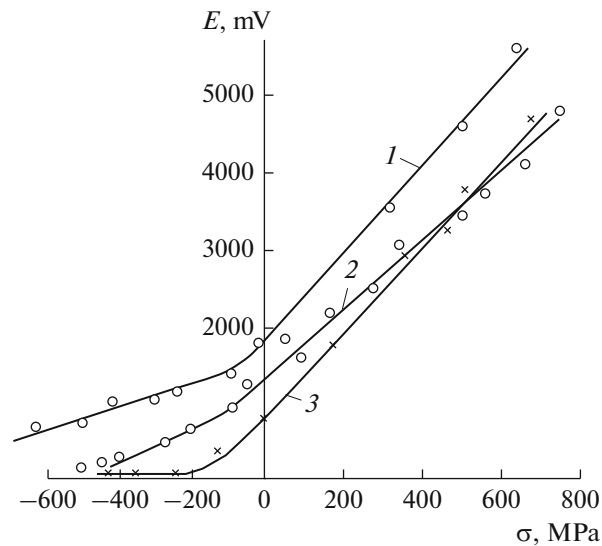


**Fig. 3.** Dependence of  $E$  on the value of mechanical stresses during wedging and compression of 03H17K10B10MT steel rings subjected to different heat treatments: (1) quenched; (2, 3) aged in different modes.

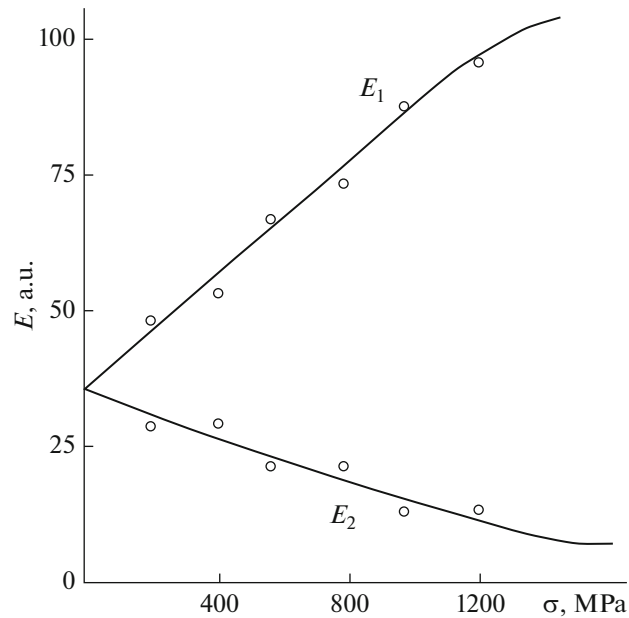


**Fig. 4.** Dependence of MN emf in steel 35 on applied stresses.

Allowing for the fact that under uniaxial loading, the deformations along and across the loading axis are related to each other by the Poisson ratio ( $\nu$ ), which is close in value to 0.3, one can conclude that it is the crystal deformation that affects the domain structure of a ferromagnet and leads to changes in the MN parameters. These conclusions are illustrated by Fig. 4, viz., elastic tensile deformations in the magnetization-reversal direction increase the MN emf ( $E_1$ ) while compressive deformations reduce the MN emf ( $E_2$ ).

Using magnetic noises made it possible to resolve a number of issues related to improving the techniques of manufacturing vital parts based on paced testing of technological residual stresses, a methodology which may prove useful when solving production problems and are of interest to specialists [5, 7, 8, 19, 20].

Good prospects for using MN in evaluating the condition of pipelines have been mentioned in [6, 7, 9, 15–17]. The following two problems should be singled out in pipeline testing:

- assessing the stressed state of steel (**A**);
- estimating the degree of steel destruction (**B**).

**A.** Straight pipeline sections (with lengths of 20 outer pipeline diameters and more) operating under product pressure and external actions are the easiest to evaluate. These zones experience the least load, and, being in the least stressed state, they are usually selected to calibrate devices.

The simplest technique of evaluating mechanical stresses in pipelines (shells) is given in [5, 8, 20]. It consists in scanning the pipeline surface along a generatrix  $\ell$  with a transducer and detecting a zone in the pipeline metal with the maximum MN emf. It is this zone that is most prone to destruction [5]. However, this technique is laborious and involves scanning generatrices  $\ell$  along all the directions of the pipeline circumference while the parameter  $E$  has only a limited sensitivity toward changes in mechanical stresses. Figure 4 shows results of measuring MN emf during magnetization reversal in the longitudinal  $E_1$  and transverse  $E_2$  directions with respect to the loading axis. The parameter  $\gamma = E_1/E_2$  can be seen to be more sensitive to stresses than  $E$ .

In this case, the technique of evaluating mechanical stresses is based on measuring the MN emf in the longitudinal and transverse magnetization-reversal directions with respect to the pipeline loading axis.

In doing so, one needs to perform magnetization reversal in two mutually orthogonal directions in pipeline metal and register the MN emf in each direction, viz.  $E_1$  for magnetization reversal along the pipeline axis and  $E_2$  for magnetization reversal across the axis, namely, in a circumferential direction.

In this case, we can write [7, 20]

$$\begin{aligned}\sigma_{1i} &= Pd[(E_{1i} - E_0) + \nu(E_{2i} - E_0)]/2h(E_2 - E_1)(1 - \nu), \\ \sigma_{2i} &= Pd[(E_{2i} - E_0) + \nu(E_{1i} - E_0)]/2h(E_2 - E_1)(1 - \nu),\end{aligned}\quad (3)$$

where  $E_{1i}$  and  $E_{2i}$  are the MN emf values in the test zone under magnetization reversal in the axial and circumferential directions, respectively;  $\sigma_{1i}$  and  $\sigma_{2i}$  are axial and circumferential stresses, respectively, at the  $i$ -th pipeline point;  $P$  is the product pressure in the pipeline;  $d$  is the pipeline diameter;  $h$  is the thickness of the pipeline wall in the test zone; and the value of  $E_0$  is determined from the relationship

$$E_0 = E_1 + \nu(E_2 - E_1)/(1 + \nu). \quad (4)$$

It can be seen from the expressions in Eqs. (3), (4) that one only needs to measure MN emf in the calibration zone ( $E_2$  and  $E_1$ ) and in the test zone ( $E_{1i}$  and  $E_{2i}$ ) in order to determine elastic mechanical stresses acting in the pipeline. The actual values of the product pressure in a straight section of the pipeline wall in the test zone are determined when measuring  $E_2$  and  $E_1$ .

The results of testing will extend to include pipeline sections that are made of the same metal and using the same technology as for metal in the calibration zone. The identity of properties is estimated either from the design documentation or by determining the chemical composition of steel and the hardness and thickness of the pipeline wall with the known techniques of nondestructive testing [7].

Implementing this technique of evaluating mechanical stresses in a pipeline involves scanning a considerable zone of its surface with concurrent alteration of the magnetization-reversal direction. In essence, the plane stressed state of the pipeline section is tested.

A magnetic-noise device *MSh-3* with a three-coordinate PC-controlled scanning attachment [19] was developed to evaluate mechanical stresses on a plane.

The *MSh-3* device and the scanner provided the possibility for scanning the pipeline surface with a prescribed pitch while changing the magnetization-reversal direction with respect to the axes of principal mechanical stresses.

**B.** The main factors that lead to pipeline destruction in local areas include growth of dislocation density (strength reduction), formation of pores and microcracks, and metal corrosion. The predominant factors that also bring closer the onset of the destruction process are mechanical stresses acting in the given local area of pipeline metal.

One should select the following local zones for pipeline evaluation [7, 15, 16]:

- stretches with the maximum stress levels (see item A above);
- stretches of pipeline sagging under such loads as soil motions, underwater passages, and so on;
- stretches in zones of pipeline's soil-to-surface exits;
- cross-sections in the least-curvature zones.

Searching for criteria of evaluating the limiting state of steel constructions never stops, as no universally recognized criterion exists at the moment that would allow one to determine the state of metal in an actual construction and to decide on its remaining service life. In this connection, there are no methods for reliable nondestructive testing of the actual state of loaded steel constructions, including pipelines.

Some normative documents currently in force specify the state of metal yield point, which is identical to the state of samples under the action of a stress ( $\sigma_{0.2}$ ) that corresponds to the 0.2% permanent deformation of metal, as the limiting state. In other documents, the limiting state is defined to be identical to the state of a sample acted upon by a stress that corresponds to the metal ultimate strength ( $\sigma_{us}$ ). The relative deformation of the sample under this stress is a mechanical characteristic of the metal and is called (relative) elongation or contraction.

Steels with elongation values within the limits of 20–25% are used for pipeline construction. These figures indicate that within the range of plastic deformations of up to 25%, the steel construction still functions properly. Therefore, evaluation criteria based on the steel yield point allow one to make use of the deformation potential of steel and those based on the ultimate strength make it possible to allow for the admissible steel deformation that still ensures proper functioning of metal. Given the above, one can assume that a more accurate criterion belongs to an intermediate region of relative deformations in between the above two stress values.

As the degree of deformation in material increases, dislocation reactions initiate formation of such bulk defects as pores and microcracks (irreversible flaws). Formation of these flaws within and in between grains in the course of metal deformation (the so-called destruction) leads to reduction of the density of metal and to a qualitative change of its state.

The emergence of destruction in metal can be characterized by the value of plastic deformation for which an inflection point (“destruction point”  $D$ ) is observed on the “true stress–deformation” curve.

A replacement of the mechanical state of metal under plastic deformation, when metal passes from a plastic state into a plastically destructive state, occurs near this point.

Figure 5 shows an example of the destructive diagram that can be used to determine the destruction point of steel 30 under its plastic deformation.

It can be seen from the “stress–deformation” curve that as deformation grows the true stress increases and a break occurs for values that correspond to point  $D$ . It should be noted that deformation near destruction points is accompanied by intense steel hardening (due to deformation) and pores and microcracks can emerge there.

Rybakova [10] gave a physical explanation for the presence of two inflection points  $D_1$  and  $D_2$  on the steel stress–strain diagram. She showed that point  $D_1$  corresponds to the onset of destructive development of plastic deformation process. It was suggested to extrapolate the first linear section of the diagram for point  $D_1''$  (see Fig. 5); this will make it possible to estimate quantitatively plastic deformation unrelated to microscopic sample destructions and to determine point  $D_1$  on the linear segment  $D_0–D_1''$ , where  $D_0$  is the origin of the stress–strain diagram.

It was proposed to use a state that corresponds to a deformation for which an inflection point was observed on the loading “true stress–deformation raised to the power of  $\frac{1}{2}$ ” curve of the sample as the criterion of admissible steel destruction. Practical research showed that this inflection point is observed in a plastic-deformation range of 3–8% for different steels, with the article keeping functioning properly [7, 15].

The physical justification of the above choice of the range (according to [18]) is the fact that for microcrack nucleation to start, a stress in the dislocation-cluster head is required that can be determined using the relationship

$$\sigma \geq 2\gamma/bn, \quad (5)$$

where  $\gamma$  is the effective surface energy of the material when a microcrack is formed;  $b$  is the Burgers vector; and  $n$  is the number of dislocations in the cluster. It can be seen that the greater the number  $n$  of dislocations in the cluster, the smaller the stress  $\sigma$  that is required for microcrack formation.

Most likely, this fact pre-determines the process of formation of separate microcracks in a testing zone that corresponds to the deformation for which destruction point  $\epsilon(D)$  is registered, namely, in the steel deformation range of 3–8% where an intense process of dislocation formation develops even if the material can still fulfill its service functions.

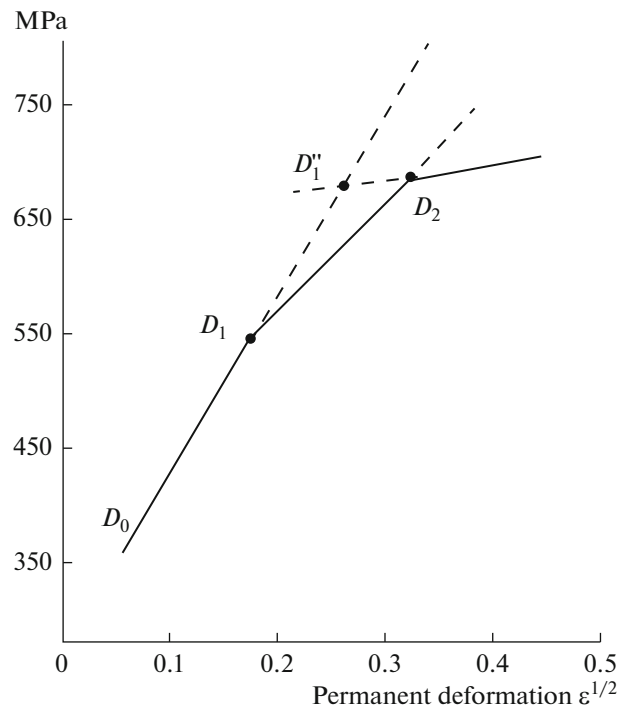


Fig. 5. Dependence of true flow stress (MPa) of steel 30 on permanent deformation  $\epsilon$  in tension.

In this connection, it is reasonable to use a state of the steel pipeline material at the degradation stage after point  $D_1$  (see Fig. 5) as the in-service limiting state. For particular grades of steel, this state can be determined from the amount of plastic deformation of samples that corresponds to the first destruction point  $\epsilon(D)$ .

The values of the relative elongation  $\epsilon(D)$  for which destruction point  $D_1$  is observed for the studied pipe steels were determined by the above technique and are listed in Table 1 [7, 17].

If the value of elongation is expressed as percentage (multiplied by 100) for the tested steels, it can be seen that destruction in these steels emerges for the plastic deformation of 3–5%.

Research has shown that dislocation processes that occur in the plastic deformation of a steel are accompanied by changes in its magnetic properties [2, 11, 12, 14]. This causes changes in the steel domain structure (internal microstresses  $\sigma_x$  increase as the dislocation density grows) and, as a result, the steel coercive force ( $H_c$ ) increases and  $e(t)$  MN decreases [2, 4, 5].

It should be expected that destruction (appearance of irreversible flaws) in steel must be accompanied by changes in its magnetic properties, specifically by the decrease of the sizes of magnetic domains (the increase of the number of domains) and, as a consequence, by the increase of the coercive force  $H_c$  and the decrease of the MN emf.

The authors of [11–14] carried out significant research into interrelation of physical processes that develop during plastic deformation with changes in the magnetic texture of steels. Peculiarities in the behavior of magnetic characteristics of steels under different modes of elastic and plastic deformation were studied. In [12, 13], it was shown that there are “breaks” on three linear segments of the coercive force dependence  $H(\epsilon^{1/2})$  that are similar to the “breaks” and the deformation curve in Fig. 5.

In what follows, we provide research results that make it possible to propose the coercive force as a parameter for evaluating the degree of destruction of steel pipelines.

Table 1

Steel grade	Steel 20	St3	09Г2С	17Г1С
Relative deformation at destruction point $\epsilon(D)$	0.048	0.033	0.036	0.04

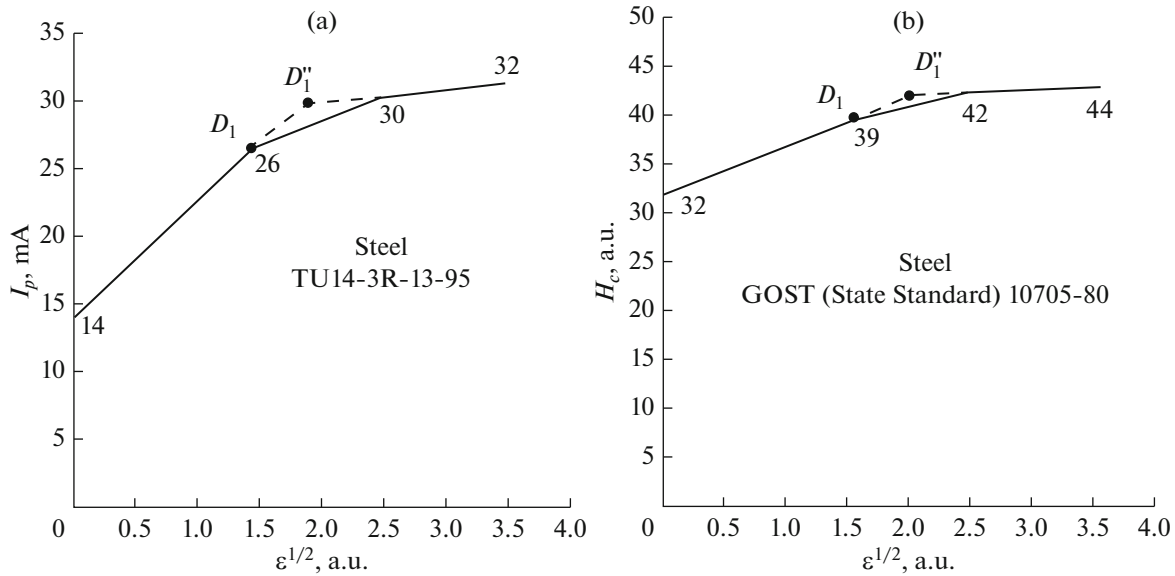


**Fig. 6.** Variation of the coercive force  $I_p(H_c)$  in the function of plastic deformation  $\epsilon^{1/2}$ : (a) in TU14-3R-13-95 steel sample as measured with the KIFM-1 device; (b) in GOST (State Standard) 10705-80 steel sample as measured with the IKM-02Ts device.

It follows from the destruction diagram in Fig. 5 that  $\sigma_x \sim \epsilon^{1/2}$  has a linear dependence. Substituting this dependence into the expression in Eq. (2), we obtain

$$H_M = \frac{2\alpha\lambda_{100}\epsilon^{1/2}}{\sqrt{K_{\text{eff}}}}. \quad (6)$$

In many works, it is pointed out that the value  $H_M$  of the maximum level of magnetic noises  $e(t)$  MN (see Figs. 1 and 2) corresponds to the coercive force  $H_c$  of the ferromagnet material [4, 5, 9]; therefore, from Eq. (6) we can qualitatively write down

$$H_c \approx H_M \sim \epsilon^{1/2}, \quad (7)$$

this defines a linear dependence  $H(\epsilon^{1/2})$  between the indicated quantities.

In practice, the state of different plasticity of steel is modeled by a preliminary plastic deformation of samples according to the standard strain-ageing techniques. According to this, carbon steel samples subjected to strain ageing were tested. Samples of three steel grades (with a carbon content of approximately 0.2%) manufactured by different technologies were used and had thicknesses of 4, 6, and 8 mm. The ageing of the samples was performed according to GOST (State Standard) 7268-82 by stretching while ensuring the permanent elongation of 2, 6 and 12% [7, 15, 17]. The coercive force was measured using KIFM-1 and IKM-02Ts devices. The results of measurements were averaged over the readings from no fewer than five samples.

Figures 6a and 6b show graphs as a function of the coercive force depending on the value of the relative plastic deformation raised to the power of  $1/2$ . It can be seen that regardless of the steel grade and the device used, the coercive force increases practically linearly on separate segments as the plastic-deformation value raised to the power of  $1/2$  increases. We thereby confirmed the possibility of employing the magnetic characteristic  $H_c$  of steel as an informative parameter in nondestructive evaluation of the degree of destruction of steel articles using the method [10] by means of extrapolation of the first linear segment of the dependence  $H(\epsilon^{1/2})$  for point  $D_1''$ .

Taking into account that the slope of the third linear segment (see Fig. 6) is insignificant, we can use the approximation  $H_c^{D''} \approx H_c^{\delta}$  when extrapolating the position of point  $D_1''$ . As the research showed, such approximation practically does not change the estimate of the resource of safe pipeline operation and makes it possible to estimate quantitatively the point of destruction.



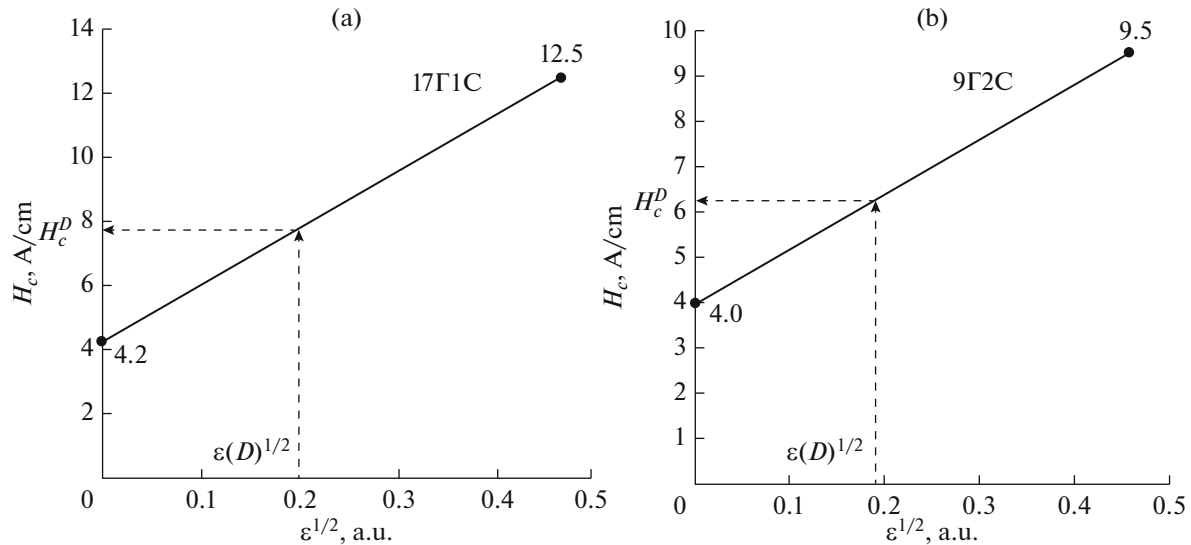


**Fig. 7.** Variation of the coercive force  $H_c$  depending on the relative deformation  $\varepsilon^{1/2}$  for (a) 17Г1С and (b) 09Г2С steels.  $\varepsilon(D)^{1/2}$  is the value of relative deformation at the steel destruction point;  $H_c^D$  is the coercive force value corresponding to the steel destruction point.

Plotting the dependence of the coercive force on the relative plastic deformation raised to the power of  $1/2$  makes it possible to determine the degree of destruction of the pipeline steel, including the resource of safe service of metal, from the actual value of this parameter. This is done by calculating (using the coercive force) the margin to achieving the point of metal destruction.

The importance of this parameter for determining the limiting state of steel pipelines consists in the fact that the state that corresponds to the deformation degree at the destruction point can be detected on an on-load pipeline by its nondestructive testing.

In its turn, to construct this dependence [the linear function of the relationship in Eq. (7)] it suffices to know the coercive force for two values of plastic deformation of steel. For convenience reasons, one can use the values of  $H_c$  for the zero deformation, i.e., for the initial condition of steel ( $H_c = H_c^0$ ), and for testing stresses that are close to the ultimate strength, i.e., for  $\varepsilon = \delta$ . Denoting this value of coercive force by  $H_c^\delta$ , we can write down  $H_c = H_c^\delta$ . These data for the studied steels are given in Table 2.

**Table 2**

Steel	Relative deformation, $\varepsilon$	$\varepsilon(D)^{1/2}$	Coercive force $H_c$ , A/cm
Steel 20	0	0	$H_c^0 = 4.2$
	$\delta = 0.23$	0.48	$H_c^\delta = 12.4$
St3	0	0	$H_c^0 = 2.8$
	$\delta = 0.22$	0.47	$H_c^\delta = 6.4$
17Г1С	0	0	$H_c^0 = 4.2$
	$\delta = 0.22$	0.47	$H_c^\delta = 12.5$
09Г2С	0	0	$H_c^0 = 4.0$
	$\delta = 0.21$	0.46	$H_c^\delta = 9.5$

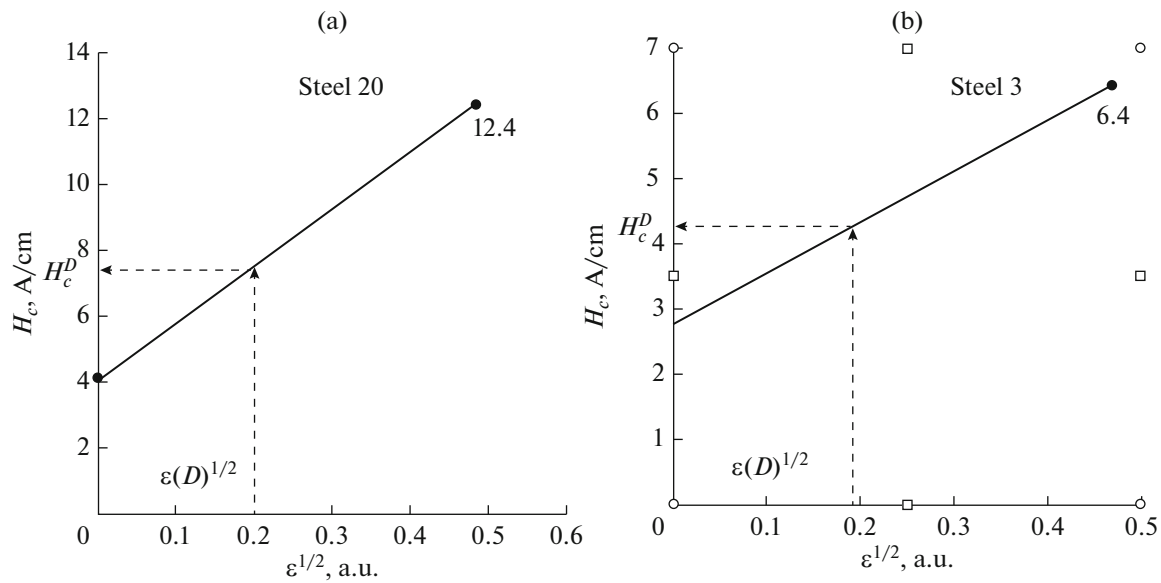


**Fig. 8.** Variation of the coercive force  $H_c$  depending on the relative deformation  $\varepsilon^{1/2}$  for (a) steel 20 and (b) steel 3.  $\varepsilon(D)^{1/2}$  is the value of relative deformation at the steel destruction point,  $H_c^D$  is the value of coercive force corresponding to the steel destruction point.

Figures 7 and 8 show the interconnection between  $H_c$  and deformation degree for four pipe steels. Straight lines were constructed based on the data of measurements of  $H_c$  on as-received samples ( $H_c^0$ ) and for stresses that correspond to the ultimate strength of steel ( $H_c^\delta$ ). The dashed line in the graphs indicates the technique of determining the limiting value of the coercive force ( $H_c^{D''}$ ) for this steel grade that corresponds to the relative deformation at the destruction point  $\varepsilon(D)^{1/2}$  that was determined for each steel based on the data provided in Table 1.

If nondestructive testing produces the values of coercive force within the limits  $H_c^0 \sim H_c^D$ , a conclusion is drawn about the operability of metal in the pipeline section. For  $H_c > H_c^D$ , the pipeline section is subjected to repair and additional testing.

The limiting values of the coercive force  $H_c^D$  were determined graphically for all the studied pipe steels. Some of the data are presented in Table 3, which shows the results of measurements of the coercive force in the initial state of steels ( $H_c^0$ ) and for a deformation that corresponds to their ultimate strength ( $H_c^\delta$ ).

Based on the dynamics of changes in the coercive force of steel  $H_c$  in a zone to the maximum in-service destruction of metal and the data on the value of the coercive in the initial state of steel and combined with other arrangements, one can evaluate the resource of safe operation of pipeline metal [7].

The possibility has thus been demonstrated for using the MN method for testing the stressed state of pipelines, specifically for evaluating the mechanical stresses and strength state of metal. The results obtained, which are partly described in [7, 15, 16], are being used for testing pipes in oil and gas industry.

**Table 3**

Steel grade	Steel 20	St3	17Г1С	09Г2С
Coercive force $H_c^D$ at destruction point $D$ , A/cm	7.5	4.3	7.9	6.2
Coercive force $H_c^0$ in as-received state, A/cm	4.2	2.8	4.2	4.0
Coercive force $H_c^\delta$ for ultimate-strength deformation, A/cm	12.4	6.4	12.5	9.5

## REFERENCES

1. *Starenie splavov* (Ageing of Alloys), Mirkina, L.I. and Zakharova, M.I, Eds., Moscow: Gos. Nauchno-Tekh. Izd. Lit. Chernoi Tsvetn. Metall., 1962.
2. Vonsovskii, S.V., *Sovremennoe uchenie o magnetizme* (Modern Concept on Magnetism), Moscow: Gos. Izd. Tekh. Lit., 1952.
3. Klyuk, B.A., Stoyakov, V.M., and Timerbulatov, G.N., *Prochnost' i remont uchastkov magistral'nykh truboprovodov v Zapadnoi Sibiri* (Strength and Repair of Segments of Gas-Main Pipelines in Western Siberia), Moscow: Mashinostroenie, 1994.
4. Gorkunov, E.S., Dragoshanskii, Yu.N., and Mikhovski, M., Barkhausen effect and its use in the structuroscopy of ferromagnetic materials (a review): Ch. 1–5, *Defektoskopiya*, 1999, no. 6, pp. 3–23; no. 7, pp. 3–32; no. 8, pp. 3–25; no. 12, pp. 3–24; 2000, no. 6, pp. 3–38.
5. Filinov, V.V., *Metody i pribory kontrolya mekhanicheskikh napryazhenii na osnove ispol'zovaniya magnitoakusticheskikh shumov* (Methods and Devices for Evaluation of Mechanical Stresses Based on the Use of Magnetoacoustic Noises), Moscow: Mashinostroenie, 2000.
6. Dubov, A.A., Demin, E.A., Milyaev, A.I., and Steklov, O.A., Experience of testing stressed-strained state of a pipeline using the magnetic memory method and its comparison with traditional methods and tools of stress evaluation, *Kontrol'. Diagn.*, 2002, no. 4, pp. 53–56.
7. Kuznetsov, N.S. and Kuznetsov, A.N., *Diagnostika truboprovodov* (Testing of Pipelines), Krasnogorsk: Zverev Krasnogorsk Zav., 2009.
8. Filinov, V.V. and Filinova, A.V., Evaluation of mechanical stresses in steel articles based on the registration of magnetic and magnetoacoustic magnetization-reversal noises, *Kontrol'. Diagn.*, 2007, no. 2, pp. 41–44.
9. Kuznetsov, A.N., On the diagnostics of the state of metal in in-service pipelines. Devices and systems. Management, *Kontrol'. Diagn.*, 2012, no. 2, pp. 55–57.
10. Rybakova, L.M., Destruction of metal under volume and surface plastic deformation, *Metalloved. Term. Obrab. Met.*, 1980, no. 8, pp. 17–22.
11. Kuleev, V.G. and Gorkunov, E.S., Mechanisms of the influence of stress on coercive force of ferromagnetic steels, *Defektoskopiya*, 1997, no. 11, pp. 3–18.
12. Kuleev, V.G., Tsar'kova, T.P., and Nichipuruk, A.P., Specific features of the behavior of the coercive force in low-carbon plastically deformed steels, *Russ. J. Nondestr. Test.*, 2005, vol. 41, no. 5, pp. 285–295.
13. Khristenko, I.N. and Krivova, V.V., Effect of plastic deformation on coercive force of low-carbon steels, *Defektoskopiya*, 1984, no. 6, pp. 90–92.
14. Kuleev, V.G., Tsar'kova, T.P., Nichipuruk, A.P., Voronin, V.N., and Berger, I.F., On the origin of essential differences in the coercive force, remanence, and initial permeability of ferromagnetic steels in the loaded and unloaded states upon plastic tension, *Phys. Met. Metallogr.*, 2007, vol. 103, no. 2, pp. 131–141.
15. Kuznetsov, A.N., Analysis of the limiting state of pipelines, *Gazov. Prom-st.*, 2012, no. 6, pp. 64–67.
16. Kuznetsov, A.N., Studying the effect of bends in pipelines on their longevity, *Gazov. Prom-st.*, 2012, no. 2, pp. 59–61.
17. Kuznetsov, A.N., Studying the effect of plastic deformation on coercive force of steel, *Prom. ASU Kontrolyer*, 2012, no. 9, pp. 60–62.
18. Krasovskii, A.Ya., *Fizicheskie osnovy prochnosti* (Physical Basics of Strength), Kiev: Naukova Dumka, 1977.
19. Filinov, V.V. and Arakelov, P.G., Developing new informative parameters for testing the stressed state of ferromagnetic materials based on registering magnetic magnetization-reversal noises, *Kontrol'. Diagn.*, 2013, no. 5, pp. 28–31.
20. Filinov, V.V., Shaternikov, V.E., and Arakelov, P.G., The monitoring of technological stresses by the method of magnetic noise, *Russ. J. Nondestr. Test.*, 2014, vol. 50, no. 12, pp. 748–759.

*Translated by V. Potapchouck*